Electronic Supplementary Information

High performance self-heated membrane distillation system for energy efficient desalination process

Subrahmanya TM [a], Po Ting Lin[*b], Yu-Hsuan Chiao[c], Januar Widakdo[a], Cheng-Hsiu Chuang[b], Shaneza Fatma Rahmadhanty[b], Shiro Yoshikawa[d], Wei-Song Hung[*a]

[a]Advanced membrane materials research center, Graduate Institute of Applied science and Technology, National Taiwan University of Science and Technology, Taipei, 10607, Taiwan.

[b]Department of mechanical engineering, National Taiwan University of Science and Technology, Taipei, 10607, Taiwan.

[C]Department of Chemical Engineering, University of Arkansas, Fayetteville, Arkansas,72701, USA.

[d]Department of Chemical Engineering, Graduate School of Science and Engineering, Tokyo Institute of Technology, Japan.

*Corresponding author: wshung@mail.ntust.edu.tw, potinglin@mail.ntust.edu.tw

1. **Digital pictures of self-heated VMD module and the experimental setup used to evaluate VMD performance of Graphene$_x$-PVDF$_1$ flat sheet membrane joule heaters:**

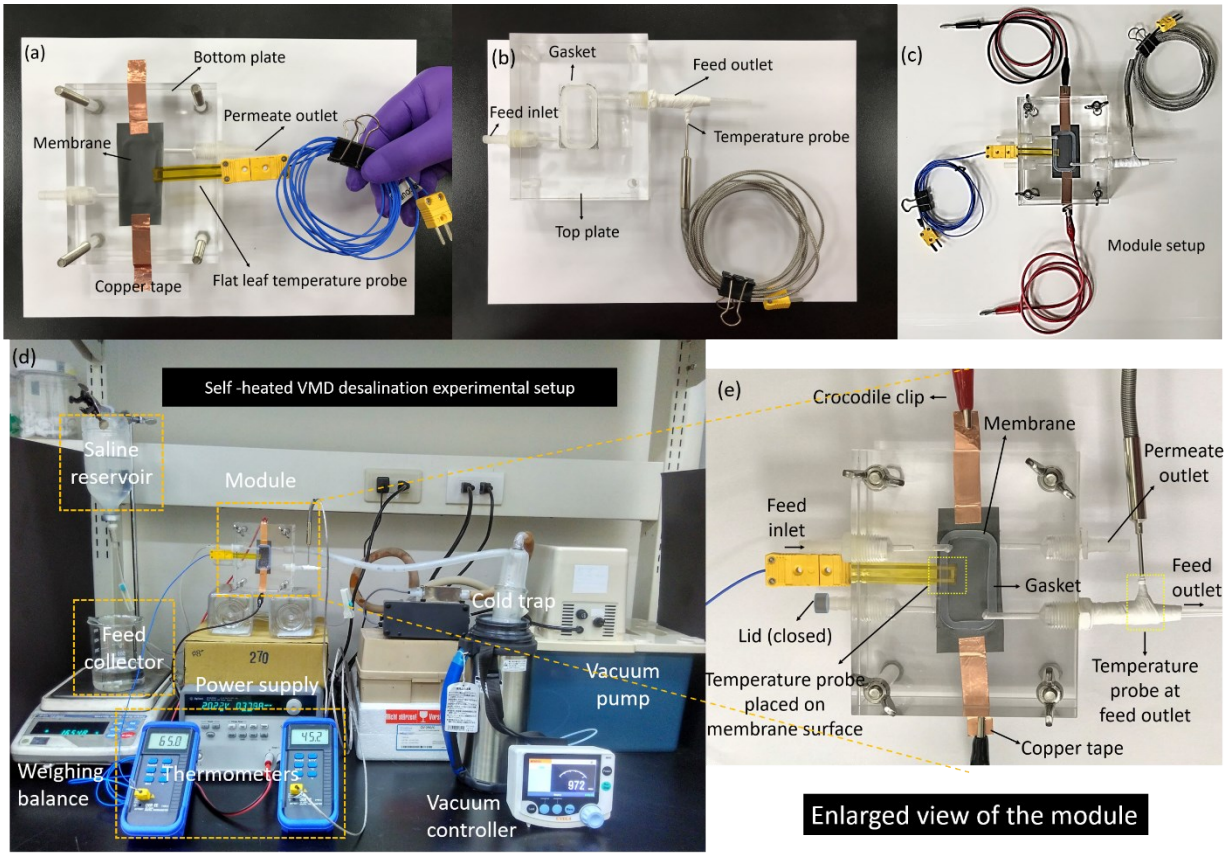

Figure. S1 a) Digital image showing the bottom plate of the module with the membrane and the flat leaf thermocouple. b) Digital image showing the top plate of the module with the thermocouple inserted to the fed outlet. c) Digital image of the module assembly and other components connected to the module. d) Digital photo of the self-heated VMD desalination setup. E) Enlarged view of the self–heated VMD module with other components.

2. a) Preparation of PDMS treated PET nonwoven support layer for Graphene$_x$ –PVDF$_1$ flat sheet membrane joule heaters and water contact angle measurements:

PDMS polymer (10g) and curing agent Sylgard 184A (1g) were dissolved in 1000 mL of THF solvent, by stirring for 12hrs using magnetic stirrer to obtain a homogeneous solution. Then the solution was transferred into a clean tray, and PET nonwoven fabric was immersed into it for 20min. After 20min, the fabric was removed from the solution and transferred to a hot air oven for drying at 120^{o}C for 1.5 hours. The superhydrophobicty of as obtained PDMS coated PET nonwoven support layer was confirmed by water contact angle measurements, while the surface functionality was confirmed by FT-IR spectroscopy.

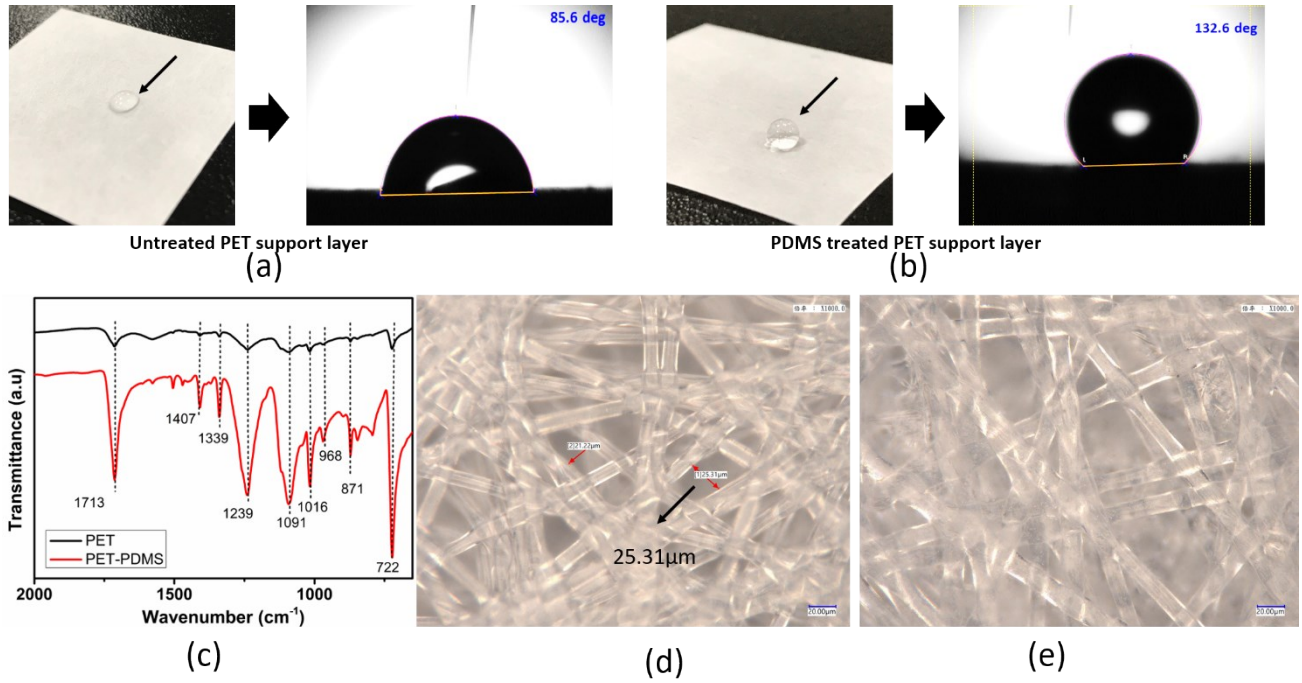

Supplementary Figure S2a: a) Water contact angle of untreated PET nonwoven support layer and b) PDMS treated PET nonwoven support layer. c) FT-IR spectra of PET nonwoven support layer and PDMS treated PET nonwoven support layer. d) Digital microscopic surface image of untreated PET nonwoven support layer. e) Digital microscopic surface image of PDMS treated PET nonwoven support layer.

The FTIR spectra of neat PET nonwoven fabric and PET-PDMS nonwoven fabric support layer (Figure.1a) were recorded in the range of 4000-650cm^{-1}, to confirm surface functionality. No prominent peak was found from 4000 to 2000cm^{-1}, except the peak at 2967cm^{-1} corresponding to C-H stretching vibration of –CH_2. Whereas for PET several peaks observed within 2000 to 600cm^{-1}. The strong peak found at 1713cm^{-1} corresponds to C=O stretching vibration; the peak at 1407cm^{-1} corresponds to aromatic skeletal stretching vibration. The peaks at 1339cm^{-1} and 1016cm^{-1} were correspond to carboxylic

stretching and anhydride stretching vibrations respectively. The absorption peaks at 1239cm^{-1} and 1091cm^{-1} were correspond to C-O-C asymmetric stretching vibration and O-C stretching vibration respectively. The peak at 968cm^{-1} represents O-CH2 and O=C-O stretching; the peak at 871 corresponds to out of plane vibration of C-H bending mode. The peak at 847cm^{-1} represents different bending modes of vibration of benzene ring. The prominent absorption peak at 722cm^{-1} represents CH_2 rocking vibration. The slight enhancement in the intensity of peaks at 1059cm^{-1} and 791cm^{-1}, after PDMS coating can be assigned to asymmetric and symmetric stretching vibration of Si-O-Si of PDMS. However, the spectrum of PET-PDMS nonwoven fabric appear almost similar to neat PET nonwoven fabric. Figure. 1 b, c shows the water contact angle of b) neat PET nonwoven fabric and c) PET-PDMS nonwoven fabric support layer. After coating PDMS, the contact angle increased from 85.6^{o} to 132.6^{o}. Thus, confirmed the superhydrophobicty of PET-PDMS nonwoven fabric[1, 2], The superhydrophobicity for support layer is necessary to avoid membrane wetting by vapor condensation since it can hinder vapor transportation across the membrane. Also support layer provides good mechanical strength to the membrane.

b) Characterization of Few-layer graphene used in the fabrication of membrane joule heaters:

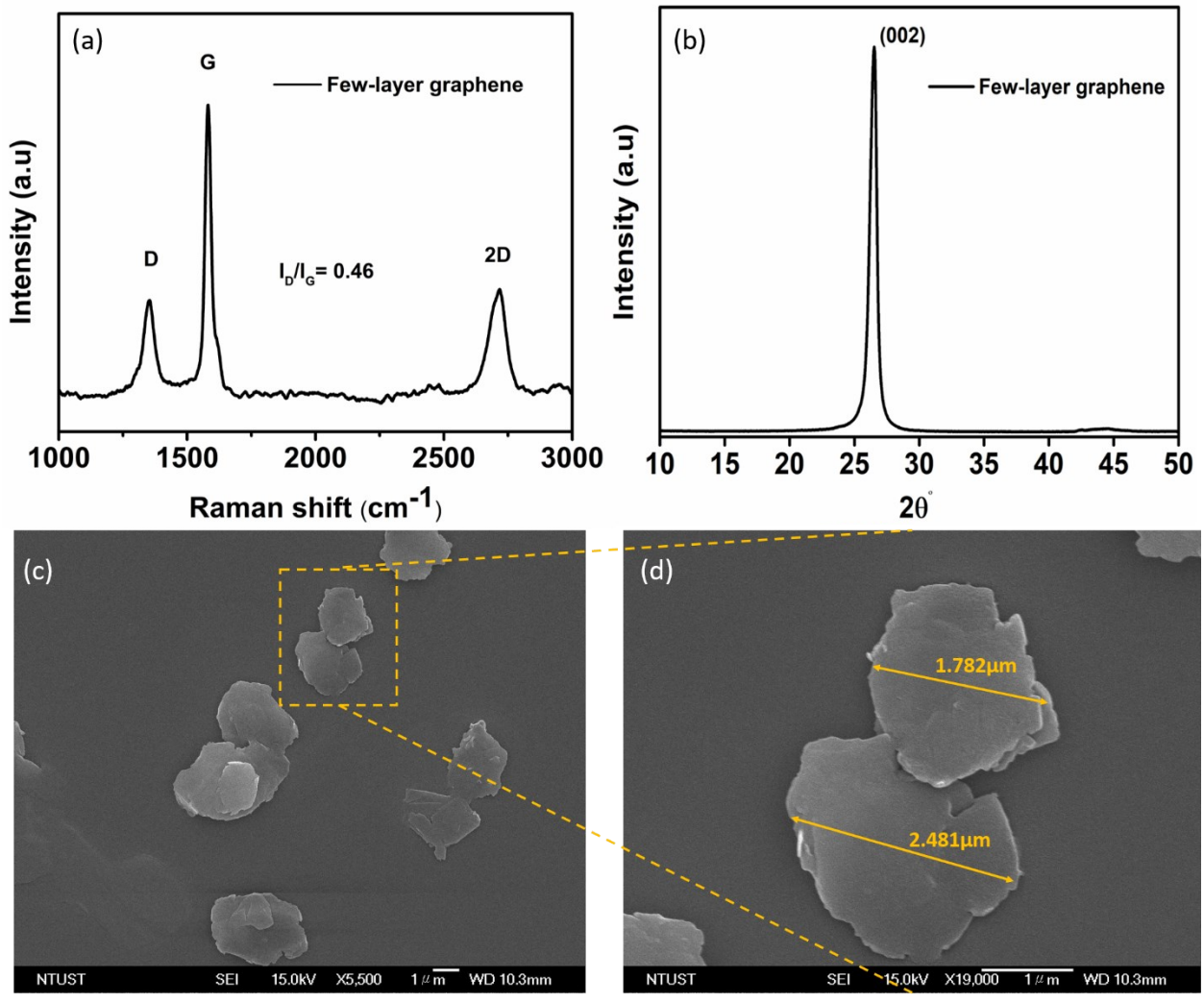

Figure. S2b: a) Raman spectra of Few -layer graphene, b) X-ray diffraction of few layer graphene, c) and d) SEM images of Few -layer graphene.

The prominent peak at 2θ =26.63°, corresponds to (002) lattice plane of few layer graphene (Figure. 2a), while the Raman spectra of few layer graphene (Figure. 2b) shows the D band peak at 1355 cm^{-1} assigned to out of plane vibrations confirming the presence of structural defects in graphene; the G band peak at 1580 cm^{-1} is attributed to in-plane vibrations of sp2 carbon atoms of graphene. While the symmetric 2D band peak at 2722 cm^{-1}can be attributed to the presence of few- layer graphene[3]. SEM image (Figure. 2c) of few layer graphene shows petal like graphene flakes with lateral size ranging between 1-3µm.

3. Determination of Bulk porosity (%) and liquid entry pressure (LEP).

The bulk porosity (%) of the as prepared membrane joule heaters containing sub-micropores was determined by the water absorbency method[4], by using the formula given below:

$$\textit{Bulk porosity (\%)} = \frac{W_{wet} - W_{dry}}{v_{dry} \times \rho_{water}} \qquad (1)$$

where, W_{dry} and W_{wet} are the membrane weights before and after immersion in water. V_{dry} is the volume of the membrane used in the dry state and ρ_{water} is the density of DI water.

The liquid entry pressure (LEP) of the membrane joule heaters was evaluated using the Cantor–Laplace equation[5] given below:

$$LEP = \frac{-2B_{\gamma L}\, COS\theta}{r_{max}} \qquad (2)$$

where, where LEP is the liquid entry pressure for pure water in Pascal (Pa), B is the dimensionless geometrical factor that includes the irregularities of the pores (B = 1 for assumed cylindrical pores), γL is the liquid's surface tension (N m^{-1}), in this case 0.07199 N m^{-1} for water at ≈ 25°C, cos θ is the water contact angle in degree, and r_{max} is the maximal pore radius (m).

Table. S1: Summary of membrane properties based on LEP and porosity.

Membrane	Surface porosity (%)	Bulk porosity (%)	LEP (Bar)
PVDF	2.1	37	0.17
Graphene1-PVDF1	3.3	65	0.86
Graphene1-PVDF1	4.4	59	2.31
Graphene1-PVDF1	9.3	41	2.44
Graphene1-PVDF1	11.2	32	2.54

4. Joule heating performance (in air medium) and VMD performance results of Graphene$_x$-PVDF$_1$ membrane joule heaters:

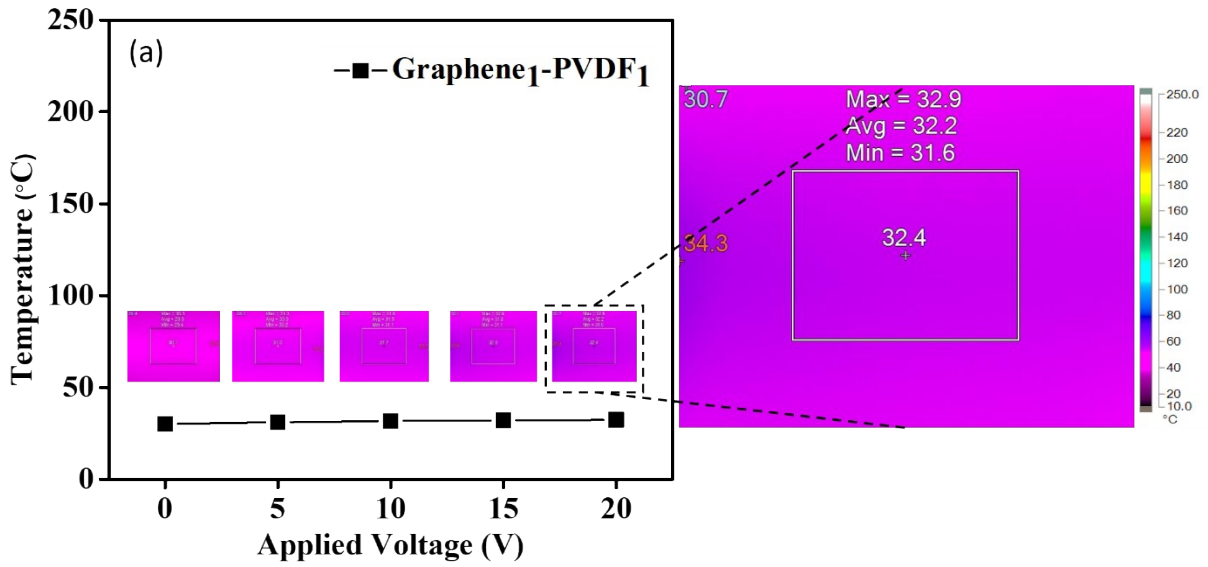

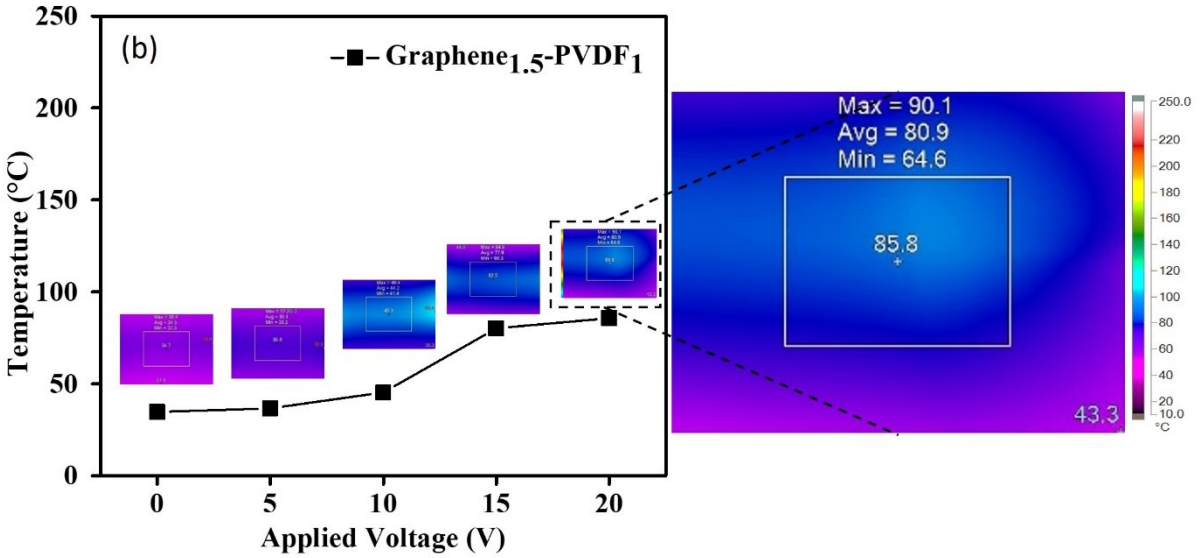
(b)
Graphene1.5-PVDF1
Temperature (°C)
Applied Voltage (V)
Max = 90.1
Avg = 80.9
Min = 64.6
85.8
43.3
°C

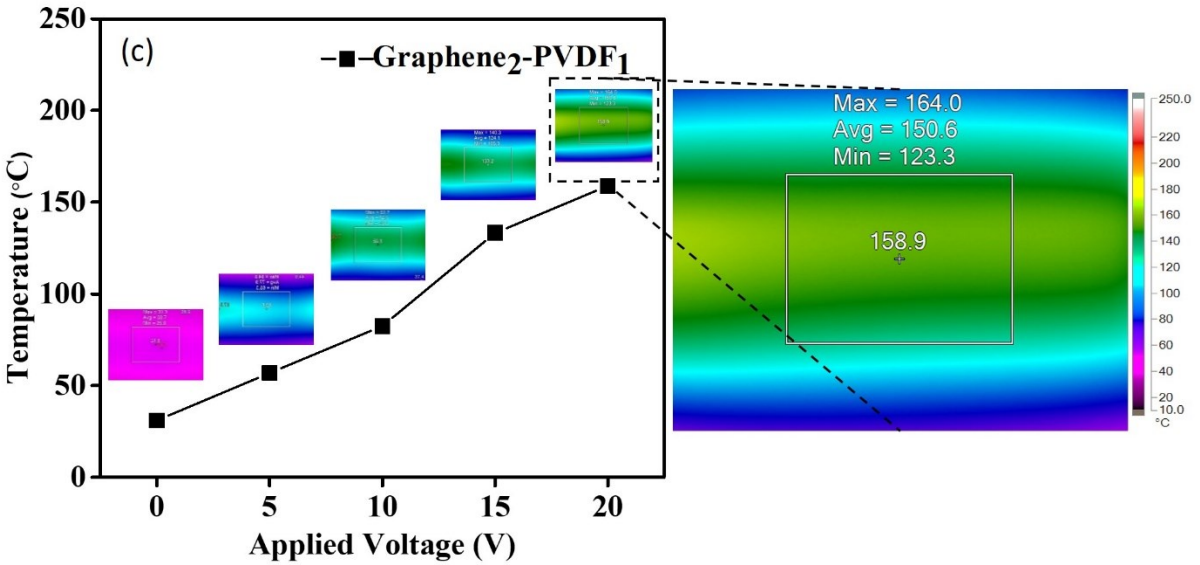
(c)
Graphene2-PVDF1
Temperature (°C)
Applied Voltage (V)
Max = 164.0
Avg = 150.6
Min = 123.3
158.9
°C

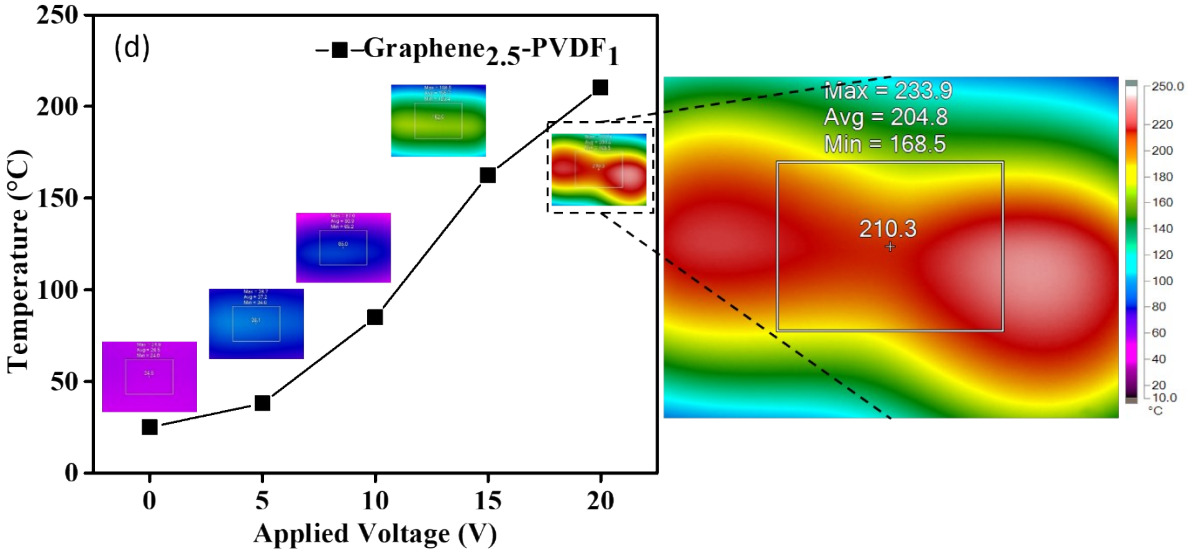

Figure. S3 Joule heating performance of Graphene$_x$-PVDF$_1$ membranes in air medium with respect to different applied voltages for; (a) Graphene$_1$-PVDF$_1$ membrane, (b) Graphene$_{1.5}$-PVDF$_1$ membrane, (c) Graphene$_2$-PVDF$_1$ membrane, (d) Graphene$_{2.5}$-PVDF$_1$ membrane.

Table. S2: Applied voltage, current and power details of different Graphene$_x$-PVDF$_1$ membrane samples for joule heating performance in air medium.

Membrane / Voltage	Graphene$_1$-PVDF$_1$		Graphene$_{1.5}$-PVDF$_1$		Graphene$_2$-PVDF$_1$		Graphene$_{2.5}$-PVDF$_1$	
	Current (I)	Power (W)	Current (I)	Power (W)	Current (I)	Power (W)	Current (I)	Power (W)
05 V	0.000 A	0.000 W	0.015 A	0.075 W	0.043 A	0.215 W	0.119 A	0.595 W
10 V	0.000 A	0.000 W	0.048 A	0.480 W	0.135 A	1.350 W	0.261 A	2.610 W
15 V	0.001 A	0.015 W	0.086 A	1.290 W	0.238 A	3.570 W	0.428 A	6.420 W
20 V	0.001 A	0.020 W	0.125 A	2.500 W	0.312 A	6.240 W	0.810 A	16.20 W

SL. NO	Membrane Sample	Voltage (V) Current (A)	FFR (mL/min)	MST- BT= ΔT ^{o}C	Flux (L/m^{2}h)	S R (%)	T P F (%)	Q_{sh} (kWh/L)	GOR
1.	$Graphene_{2.5}$-$PVDF_{1}$	20 V, 0.700 A	1.0	65.00- 45.20=19.8	28.72	99.38	143.8	0.626	1.001
			1.5	60.00- 42.00=18.0	28.19	99.50	142.9	0.638	0.983
			2.0	50.00- 36.00=14.0	27.02	99.51	138.9	0.665	0.942
			2.5	44.00- 29.00=15.0	26.36	99.52	151.7	0.682	0.919
		15 V, 0.540 A	1.0	64.00-44.60=19.4	27.12	99.41	143.5	0.383	1.634
			1.5	57.00-40.00=17.0	26.26	99.49	142.5	0.396	1.582
			2.0	49.00-34.90=14.1	23.11	99.57	140.0	0.450	1.393
			2.5	41.50-26.50=14.5	17.32	99.62	154.7	0.600	1.044

		10 V, 0.200 A	1.0	56.00-38.50=17.5	23.44	99.41	145.4	0.109	5.720
			1.5	48.00-33.00=15.0	21.11	99.46	145.4	0.121	5.150
			2.0	40.00-25.00=15.0	15.10	99.50	160.0	0.170	3.683
			2.5	34.50-22.80=11.7	07.97	99.57	153.3	0.322	1.944
2.	$Graphene_2$-$PVDF_1$	20 V, 0.500 A	1.0	62.00-43.00=19.0	28.14	99.38	144.2	0.456	1.373
			1.5	59.50-41.00=18.5	26.32	99.40	145.1	0.487	1.285
			2.0	49.00-34.40=14.6	19.63	99.50	142.4	0.654	0.960
			2.5	40.50-26.00=13.5	13.92	99.66	155.8	0.922	0.680
		15 V, 0.340 A	1.0	53.00-37.50=15.5	21.58	99.39	141.3	0.303	2.065
			1.5	48.00-33.50=15.0	20.00	99.38	144.7	0.327	1.910
			2.0	41.00-26.00=15.0	16.25	99.46	157.7	0.403	1.555
			2.5	36.00-24.00=12.0	12.16	99.56	150.0	0.538	1.163
		10 V, 0.198 A	1.0	36.00-23.00=13.0	12.50	99.27	156.5	0.200	3.084
			1.5	—	—	—	—	—	—
			2.0	—	—	—	—	—	—
			2.5	—	—	—	—	—	—
3.	$Graphene_{1.5}$-$PVDF_1$	20 V, 0.074 A	1.0	49.00-33.50=15.4	16.82	99.30	145.8	0.112	5.548
			1.5	42.50-25.00=17.5	11.79	99.34	170.0	0.161	3.889
			2.0	34.00-21.00=13.0	05.11	99.39	162.0	0.371	1.685
			2.5	—	—	—	—	—	—
		15 V, 0.054 A	1.0	43.00-26.50=15.5	09.00	99.30	162.3	0.115	5.423
			1.5	35.50-22.50=13.0	04.14	99.40	157.8	0.251	2.495
			2.0	—	—	—	—	—	—
			2.5	—	—	—	—	—	—
		10 V, 0.036 A	1.0	35.00-21.50=13.5	04.00	99.27	162.8	0.116	5.42
			1.5	—	—	—	—	—	—
			2.0	—	—	—	—	—	—
			2.5	—	—	—	—	—	—

Table. S3: VMD performance results of $Graphene_x$-$PVDF_1$ membranes with respect to different applied voltage and feed cross flow rates

Abbreviations: FFR- Feed flow rate, MST-Membrane surface temperature, SR-Salt rejection, TPF-Temperature polarization factor, Q_{sh} –Specific heating energy, GOR-Gain output ratio.

Details of GOR calculation; an example from Table S3, SL.NO. 1, for the case of $Graphene_{2.5}$-$PVDF_1$, 10 V, 0.200 A, and J_w = 23.44 L/m^{2}h.

$$GOR = \frac{J_W \times h_v}{Q_{in}}$$

Now, Q_{in} (kW/m^2) = $\frac{V \times I}{A \times 1000}$

Where, V= Volt, I= current (Ampere), and A = Effective membrane area (m^2).

And, J_w= Flux in (L/m^{2}h)

And, h_v = latent heat of evaporation for water =2256 kJ/kg

For example, In table S3, SL.NO. 1.

V= 10V & I= 0.2A, J_w = 23.44 L/m^{2}h,

& A= 0.00077854 m^2

$$\therefore Q_{in} = \frac{V \times I}{A \times 1000} = \frac{10 \times 0.2}{0.00077854 \times 1000} = 2.56891104 \text{ kW/m}^2$$

$$\& \; J_W \times h_v = 23.44 \times 2256 \; \frac{L}{m^2 h} \times \frac{kJ}{Kg}$$

For standard condition, 1Kg = 1L, & 1h = 3600 sec.

$$\therefore J_W \times h_v = 52{,}880.64 \; \frac{kJ}{m^2 h}$$

$$= \frac{52{,}880.64}{3600} \frac{kJ}{s \times m^2}$$

$$= 14.6890667 \; \frac{kW}{m^2} \quad \text{(kW= kJ/sec)}$$

$$\therefore \text{GOR} = \frac{14.6890667 \; kW/m^2}{2.56891104 \; kW/m^2}$$

$$= 5.718$$

Some of the system design and experimental factors that influence the GOR in this study.

***i. Exposed surface area of the membrane*:** Based on the module design, the effective membrane area is 0.00077854m^2. However, the actual surface area of the membrane to which the water molecules get exposed is higher than the effective membrane area, due to the high surface micro porosity and roughness of the membrane, that leaves a bigger area for the water to evaporate from, so that speeds up the process.

ii)*. Lower feed flow rate (FR)*: For self-heated MD systems lower flow rates provide higher permeate flux. Lower flow rate increases the hydraulic residence time (water-membrane contact time). Thus, provides the maximum efficiency of joule heating. Since the thickness of the bulk solution is too small (channel thickness (1.5mm) = Thickness of interface + Thickness of bulk), and the flow rate is low (ie, 2.5mL/min= 0.139cm/s, 2mL/min = 0.111cm/s, 1.5mL/min= 0.0833cm/s, and 1mL/min= 0.055cm/s), the heat energy dissipated to the bulk remains inside the feed chamber for few seconds and increases the overall bulk temperature. Subsequently, the elevated bulk temperature leads to increase in vapor pressure and therefore increases the tendency of evaporation of water molecules, as vapor pressure is exponentially related to temperature, according to Antoine's equation.

iii). *Suppressed temperature polarization (TP)*: Since, the heating was done locally at the membrane/feed interface, the localized heating focuses the energy at the boundary where evaporation occurs and wastes little energy heating the bulk water (however, lower flow rate helps to recover some of the dissipated heat from the bulk), and due to better thermal conductivity and hydrophobicity of graphene, the water molecules right above the membrane surface vaporize quickly and diffuse through the membrane and therefore overcomes thermal polarization by providing less time for water molecules to conduct heat to the bulk. Also, the presence of vapor at the membrane/feed interface also speeds up the evaporation of water molecules. Therefore, higher GOR can be attained as consumed heating energy is reduced, or the permeate flux for a certain input heating energy is increased.

Table S4: Comparison of specific heating energy (Qsh) and gain output ratio (GOR) values of some of the published self-heated MD systems with the lowest specific heating energy (Qsh) and highest gain output ratio (GOR) values obtained in this study (Relative to Fig.5).

Heating method of the system	**Heating membrane material**	**Q_{in} (kW/m^2)**	**J_W (L/m^2h)**	**Q_{sh} (kWh/L)**	**Gain Output Ratio (GOR)**	**Reference**
Joule heating	Graphene-PVDF	2.56	23.44	0.109	5.72	This Work
Induction heating	PTFE – Fe-CNTs	0.781	4	0.2	3.45	23
Photothermal	PVDF-CB NPs	1.367	6.1	0.22	2.8	16
Photothermal	PVDF-Polydopamine (PDA)- SiO_2/Au nano shells	1.367	5.8	0.24	2.66	16
Joule heating	PVDF – Nichrome resistance wire (NRW)	1.56	2	0.78	0.8	25
Photothermal	Carbonized eggshell-CNTs	1	1.15	0.87	0.72	18
Photothermal	Ag NPs-PVDF	23	25.7	0.89	0.7	13
Photothermal	Nickel foam-Graphene array	1	1.1	0.9	0.69	15
Joule heating	PTFE-(CNTs-PVA)	11.1	7.5	1.48	0.5	12
Photothermal	Electrospun PVDF-Ag NPs	3.2	2.5	1.28	0.49	14

Photothermal	PVDF-(Carbon black (CB)-PVA)	0.7	0.5	1.4	0.45	20
Photothermal	PVDF-PDA	0.75	0.49	1.53	0.41	17
Photothermal	Lens array on PVDF-CB NPs	0.7	0.33	2.12	0.3	19

5. Polynomial response surfaces with respect to the VMD experimental variables:

Each response surface was generated based on the following polynomial model:

$$f = a_1x_1^2 + a_2x_2^2 + a_3x_3^2 + a_4x_1x_2 + a_5x_2x_3 + a_6x_3x_1 + a_7x_1 + a_8x_2 + a_9x_3 + a_{10} \text{ * MERGEFORMAT (1)}$$

which could be rewritten as the following matrix form:

$$f = \begin{bmatrix} x_1^2 & x_2^2 & x_3^2 & x_1x_2 & x_2x_3 & x_3x_1 & x_1 & x_2 & x_3 & 1 \end{bmatrix} \cdot \begin{bmatrix} a_1 \\ a_2 \\ \vdots \\ a_{10} \end{bmatrix} \text{ * MERGEFORMAT (2)}$$

Each experimental data was substituted into Eq. * MERGEFORMAT (2), the following equation was then obtained:

$$\begin{bmatrix} f^{(1)} \\ f^{(2)} \\ \vdots \\ f^{(m)} \end{bmatrix} = \begin{bmatrix} (x_1^{(1)})^2 & (x_2^{(1)})^2 & (x_3^{(1)})^2 & x_1^{(1)}x_2^{(1)} & x_2^{(1)}x_3^{(1)} & x_3^{(1)}x_1^{(1)} & x_1^{(1)} & x_2^{(1)} & x_3^{(1)} & 1 \\ (x_1^{(2)})^2 & (x_2^{(2)})^2 & (x_3^{(2)})^2 & x_1^{(2)}x_2^{(2)} & x_2^{(2)}x_3^{(2)} & x_3^{(2)}x_1^{(2)} & x_1^{(2)} & x_2^{(2)} & x_3^{(2)} & 1 \\ \vdots & \vdots & \vdots & \vdots & \vdots & \vdots & \vdots & \vdots & \vdots & \vdots \\ (x_1^{(m)})^2 & (x_2^{(m)})^2 & (x_3^{(m)})^2 & x_1^{(m)}x_2^{(m)} & x_2^{(m)}x_3^{(m)} & x_3^{(m)}x_1^{(m)} & x_1^{(m)} & x_2^{(m)} & x_3^{(m)} & 1 \end{bmatrix} \cdot \begin{bmatrix} a_1 \\ a_2 \\ \vdots \\ a_{10} \end{bmatrix} \text{ *}$$

MERGEFORMAT (3)

or, it could be rewritten as:

$$\mathbf{F} = \mathbf{X} \cdot \mathbf{A} \qquad \text{* MERGEFORMAT (4)}$$

where $\mathbf{F}$ is a $m \times 1$ vector that is composed of all the responses from each experiment; $\mathbf{X}$ is a $m \times 10$ matrix that is composed of all the terms in the polynomial model evaluated with respect to the experimental variables; $\mathbf{A}$ is a 10×1 vector that is composed of all the coefficients in the polynomial model. Least Square Approximation (LSA) was then used to determine the coefficients in $\mathbf{A}$, which is given as:

$$\mathbf{A} = (\mathbf{X}^{\mathrm{T}} \cdot \mathbf{X})^{-1} \cdot \mathbf{X}^{\mathrm{T}} \cdot \mathbf{F} \qquad \text{* MERGEFORMAT (5)}$$

6. Determining the optimal temperature such that the difference between the ratio of the effective heating area of membrane and the ratio of pure water flux was minimized:

An effective heating area was defined as membrane area that has the temperature greater than a critical temperature T^*. Effective heating at the membrane surface produces effective flux of pure water. Therefore, it was desired to find the T^* such that the difference D between the effective heating area and the ratio of permeate flux was minimized. The difference D was defined as:

$$D = \left\| \mathbf{E} - \mathbf{Y} \right\| \qquad \text{* MERGEFORMAT (1)}$$

where $\mathbf{E}$ and $\mathbf{Y}$ are the normalized ratio of effective heating area of membrane and the normalized ratio of permeate flux, respectively. As a result, the optimal temperature T^* was found to be $38.0℃$. In other words, the ratio of the effective area that had the temperature greater than or equal to $38.0℃$ was the closest to the resultant ratio of permeate flux. More details about the effective heating area versus different values of critical temperature are given in the following table.

Table. S5: Effective heating area versus different values of critical temperature in each Case of experimental variables relative to the Graphene$_{2.5}$-PVDF$_1$ membrane.

Case / Critical Temp. (℃)	Case 1: 10V + 1mL/min	Case 2: 10V + 2.5mL/min	Case 3: 20V + 1mL/min	Case 4: 20V + 2.5mL/min
27.5	100.0%	100.0%	100.0%	100.0%
32.5	90.4%	74.5%	98.1%	94.8%
37.5	72.8%	32.0%	90.0%	74.1%
42.5	55.6%	12.2%	80.8%	51.8%
47.5	39.1%	0.1%	71.9%	31.2%
52.5	26.0%	0.0%	63.2%	20.2%
57.5	16.2%	0.0%	54.7%	12.1%
62.5	6.1%	0.0%	46.2%	3.9%
67.5	1.7%	0.0%	37.6%	0.1%
72.5	0.0%	0.0%	29.7%	0.0%
77.5	0.0%	0.0%	23.7%	0.0%
82.5	0.0%	0.0%	17.9%	0.0%
87.5	0.0%	0.0%	12.8%	0.0%
92.5	0.0%	0.0%	7.2%	0.0%
97.5	0.0%	0.0%	2.2%	0.0%
Optimal Temperature: 38 ℃	71.1%	30.0%	89.1%	71.9%

7. Digital photo of different Graphene$_x$-PVDF$_1$ flat sheet membrane joule heaters fabricated by nonsolvent induced phase separation method.

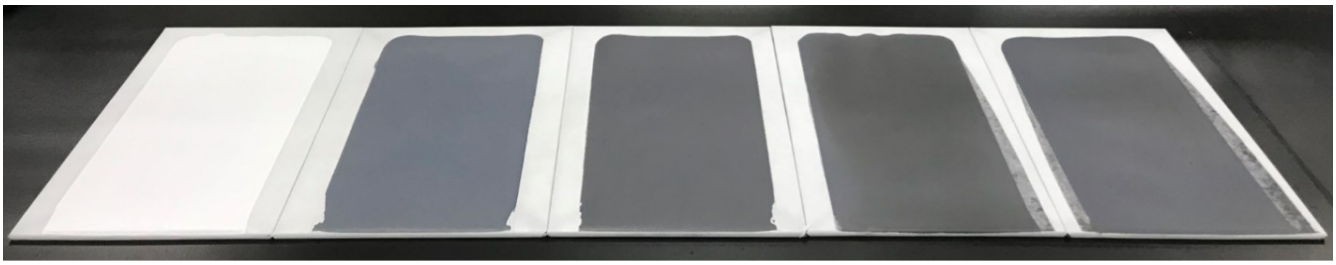

Figure S4. Digital photo of Graphene$_x$-PVDF$_1$ flat sheet membrane joule heaters.

8. Water contact angle (WCA) measurements of Graphene$_x$-PVDF$_1$ flat sheet membrane joule heaters.

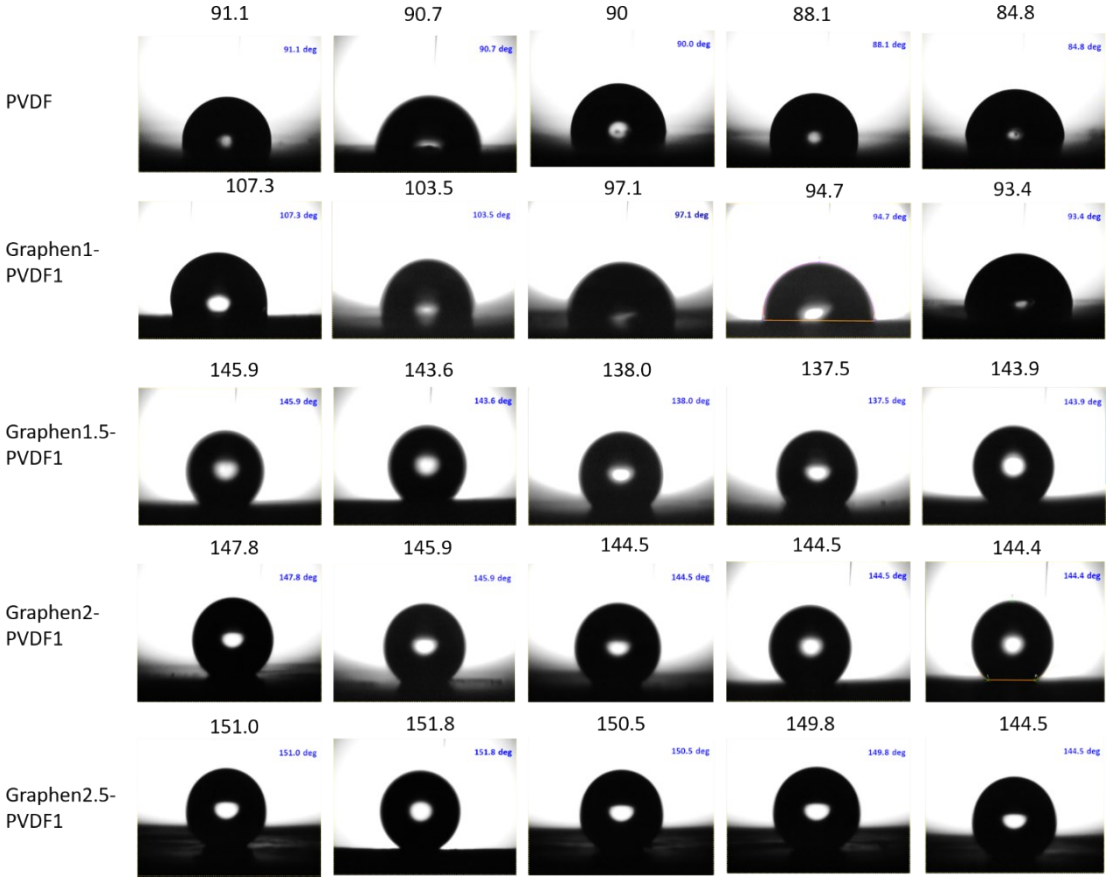

Figure S5: Water contact angle (WCA) measurements of Graphene$_x$-PVDF$_1$ flat sheet membrane joule heaters. (Five samples from each membrane joule heater were tested in order to confirm uniform hydrophobicity of the membrane joule heaters. Before WCA measurement, the water droplets were allowed for few minutes to attain stable contact angle on membrane's surface).

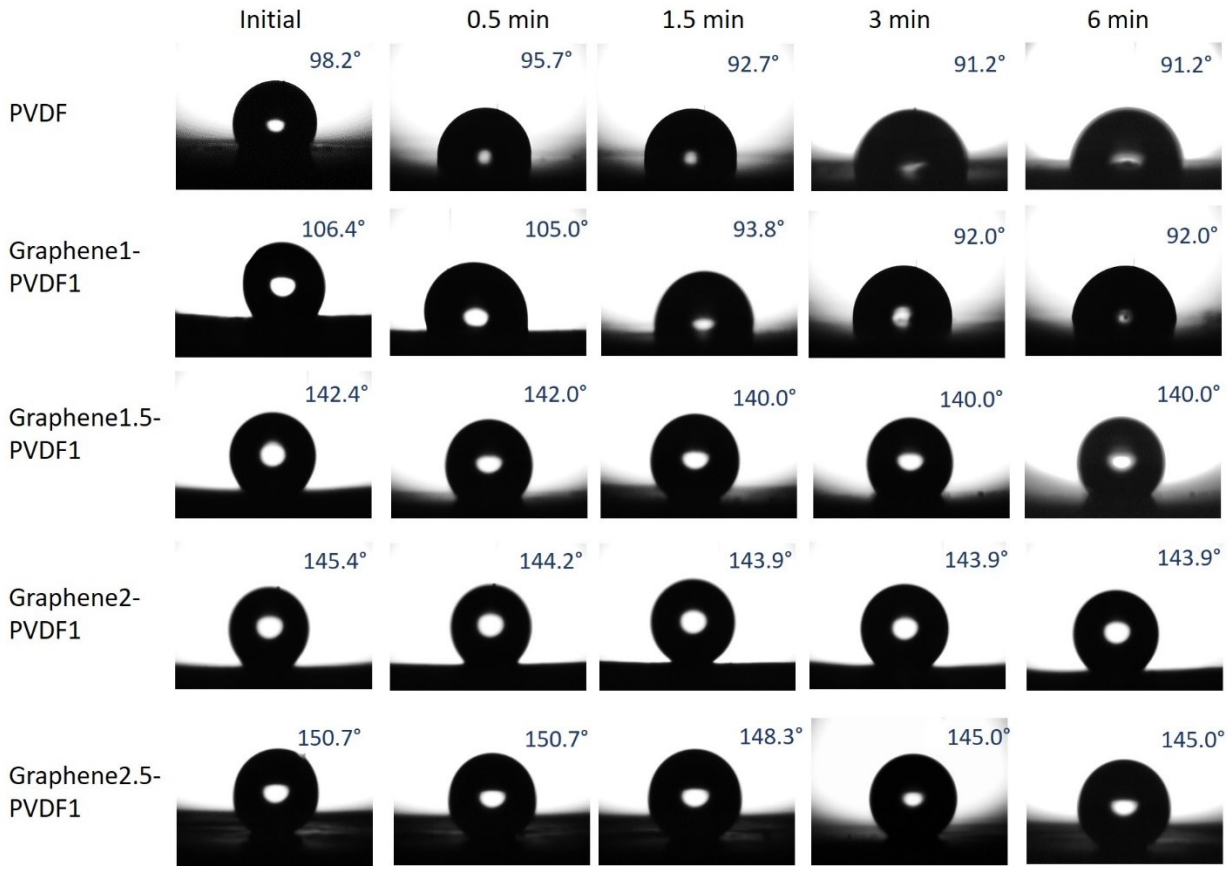

Figure S6: Different stages of water contact angles (WCAs) changing over time measurements of Graphenex-PVDF$_1$ flat sheet membrane joule heaters. (Within five minutes after coming in contact with membrane surface, the droplets attained stable WCA).

9. **Table S6**: **Conversion of volumetric flow rate to velocity flow rate.**

SL. No.	**Volumetric flow rate (mL/min)**	**Flow rate in velocity (mm/s)**	**Flow rate in velocity (cm/s)**
1.	2.5	1.389	0.1389
2.	2	1.111	0.1111
3.	1.5	0.833	0.0833
4.	1	0.555	0.0555

An example for conversion of volumetric flow rate to velocity flow rate.

$$\text{Velocity (mm/s)} = \frac{Flow\ rate}{Cross\ sectional\ area\ of\ the\ channel}$$

Now, from Table S6, SL. No 1. Flow rate= 2.5mL/min,

= 2500mm^3/min (1mL= 1000mm^3, & 1min=60 sec)

= 41.67 mm^3/sec

And, Cross sectional area of the channel (A) = width (w)×height (h)

= 20mm× 1.5mm

= 30mm^2

 Velocity (mm/s)= $\frac{41.67mm^3/sec}{30mm^2}$

= 1.389mm/sec

= 0.1389cm/sec

References

[1]. L. M. Johnson, L. Gao, C. W. Shields Iv, M. Smith, K. Efimenko, K. Cushing, J. Genzer and G. P. López, *Journal of Nanobiotechnology*, **2013**, 11, 22.

[2]. H. J. Kim, S. W. Han, J. H. Kim, H. O. Seo and Y. D. Kim, *Current Applied Physics*, **2018**, 18, 369-376.

[3]. A. C. Ferrari, J. C. Meyer, V. Scardaci, C. Casiraghi, M. Lazzeri, F. Mauri, S. Piscanec, D. Jiang, K. S. Novoselov, S. Roth and A. K. Geim, *Physical Review Letters*, **2006**, 97, 187401.

[4]. Z. Guo, R. Xiu, S. Lu, X. Xu, S. Yang and Y. Xiang, *Journal of Materials Chemistry A*, **2015**, 3, 8847-8854.

[5]. S. S. Ray, S.-S. Chen, C. T. Ngoc Dan, H.-T. Hsu, H.-M. Chang, N. C. Nguyen and H.-T. Nguyen, *RSC Advances*, **2018**, 8, 1808-1819.